



## Geochemical exploration for Li in regional scale utilizing Staged Factor Analysis (SFA) and Spectrum-Area (S-A) fractal model in north central Iran

Farshid Koohzadi<sup>1</sup>, Peyman Afzal<sup>\*2</sup>, Davood Jahani<sup>1</sup>, Mohsen Pourkermani<sup>1</sup>

1. Department of Geology, North Tehran Branch, Islamic Azad University, Tehran, Iran

2. Department of Petroleum and Mining Engineering, South Tehran Branch, Islamic Azad University, Tehran, Iran

Received 10 August 2020; accepted 17 November 2020

### Abstract

The main aim of this study was to outline the lithium anomalies by a regional exploration, at an area of 7800 km<sup>2</sup>, in Semnan province (north central Iran) using the Staged Factor Analysis (SFA) and Spectrum-Area (S-A) fractal model based on stream sediments and rock samples. Results derived via the SFA denote that Li was located in a factor as F2-4 with B, Cs, U and Rb which was utilized for calculation of the threshold values by the S-A method. The F2-4 data were classified by the fractal model for determination of the Li anomalies. Main anomaly for  $F2-4 \geq 1.5$  was situated in the SW and northern parts of this region. Furthermore, Li high grades of rock samples were correlated with main F2-4 anomalies. The main anomalies were correlated with geological particulars of Li mineralization types which represent that the main F2-4 anomalies associate with volcanic and tuff units in the SW part, and overlapped with clay minerals in the northern sector of this region. On the other hand, there are proper potential for Li mineralization which is demonstrated by this method.

**Keywords:** Lithium; Geochemical exploration; Staged Factor Analysis (SFA); Spectrum-Area (S-A) fractal model

### 1. Introduction

One of the universal strategic element is lithium as green metal for high level technologies at 21th century. Different Li sources are investigated in the world specifically pegmatite and granitic masses, brines and clay minerals (London 2008; Kesler et al. 2012). Demand for Li is increased intensively and many regional exploration projects for this metal are ongoing in many countries. Granitic and pegmatite rocks, clay minerals especially smectite and hectorite and brines occur in many parts of Iran (Fyzollahi et al. 2018; Saadati et al. 2020). Granitic-pegmatite rocks contains Be, Cs, Rb, Sc, Rare Earth Elements (REEs), W, Sn, Th and U with Li (Kesler et al. 2012). Main operation for this aim is geochemical exploration especially by stream sediments and further exploration by lithochemical samples (Kesler et al. 2012; Fyzollahi et al. 2018; Gourcerol et al. 2020). Geochemical surveys can be used for detection of post-mineralization sub-systems. The stream sediment data is an effective tool for determination of primary ore characteristics. It is more essential for exploration of rare metals such as Li (Yousefi et al. 2019). Recognition of various geochemical anomalies from background is a key process for regional scale of geochemical exploration. It have been used for definition of geochemical signatures of different ore deposit types for detailed exploration (Ostadosseini et al. 2018; Afzal et al. 2019; Mirzaei et al. 2020). Conventional statistical approaches are generated due to average, median and standard deviation such as histogram, median and box-plots.

\*Corresponding author.

E-mail address (es): [P.Afzal@azad.ac.ir](mailto:P.Afzal@azad.ac.ir)

These methods are related to distribution of variables and the spatial pattern features of the studied region including the shape, extent and magnitude of anomalous areas are not essential (Hawkes and Webb 1979; Davis 2002; Reimann et al. 2005). The spatial distribution of ore elements in stream sediments and lithochemical samples are important factors for planning of grid drilling, and structural methods such as fractal modeling can be used for this aim (Heidari et al. 2013; Daneshvar Saein et al. 2012; 2014; Daneshvar Saein and Afzal 2017; Chen and Cheng, 2018).

Fractal modeling has been applied for natural sciences after Mandelbrot (1983). The patterns of elemental grades have fractal particulars such as self-similarity on different scales and distributions (Agterberg et al. 1996). Furthermore, additional studies indicate that the different geochemical data specifically stream sediments has multifractal nature (Afzal et al. 2010; 2017a,b; Zuo 2014; Zuo and Wang, 2016; Khalili and Afzal 2018; Farahmandfar et al. 2020). Various fractal models have been improved and applied to for definition and classification of geochemical anomalies due to ore mineralization and geological phenomena by several researchers (Mandelbrot 1983; Cheng et al. 1994; Hassanpour and Afzal 2013; Afzal et al. 2017a; Chen and Cheng, 2018; Shahsavarani et al. 2020).

Multivariate analysis specifically factor analysis is an appropriate methodology to categorize and reduce the number of variables which is widely used for geochemical exploration (Zuo 2014; Yousefi et al. 2012; 2014; Afzal et al. 2017c; Ghasemzadeh et al. 2019). Yousefi et al. (2014) developed a multivariate method entitled "Staged Factor Analysis (SFA)" for classification of elemental paragenesis based on type of studied ore

deposit. This methodology used for detection of paragenesis for main ore element (Fyzollahi et al. 2018; Afzal et al. 2019).

In this study, the SFA and fractal modeling used for regional exploration of Li in the about 7800 km<sup>2</sup> of north central Iran. First, Li with other paragenesis elements were separated from others. Then, the Spectrum-Area (S-A) fractal model was applied for separation of factor anomalies related to Li. Finally, the results were correlated to further rock samples and geological particulars based on main type of Li ore mineralization.

## 2. Methodology

### 2.1. Spectrum-Area (S-A) fractal model

Fourier/inverse Fourier transformation has been generally used in time series analysis and signal processing. Spectral energy density functions illustrate the power spectrum distribution in the frequency domain. The advantage of dealing with fields in the frequency domain is that some complex convolution operations in the spatial domain for correlation analysis, filtering, and transformation can be simplified significantly in the frequency domain (Cheng 1999; Afzal et al. 2012; 2017b; Fyzollahi et al. 2018). Cheng (1999) proposed the S-A fractal model to represent the power-law frequency distribution of the power spectrum density, which is useful to separate geochemical background from anomalies. A function relating the fractal model and the spectral-energy-density function was derived to indicate the power-law relationship between the spectral-energy-density value (S) and the "area" of the set A( $\geq$ S) with spectral-energy-density values above S on the power-density plane. The model is expressed as follows (Cheng 1999; Afzal et al. 2013):

$$A(\geq S) \propto S^{-2d/s} \quad (1)$$

where 2d is related to the so-called elliptical dimension with  $d = 1$ , corresponding to isotropic dimension, and  $s > 0$ , the exponent of the power law. The power spectrum modeling modeling have been studied in different cases (Afzal et al. 2012; 2013; 2017a; Zuo 2014; Zuo and Wang 2016). This model has a main advantage in comparison with other fractal methods which is removing noise data and cells for better separation of geochemical anomalies.

### 2.2. SFA

The staged factor analysis is a multivariate analysis method based on factor analysis for extraction of significant multi-element anomalous signatures (Yousefi et al. 2014). In this approach, to recognize multi element associations in a geochemical dataset, non-indicator (noisy) elements are progressively recognized and extracted from the analysis until a satisfactory significant multi-element signature is obtained (Yousefi et al. 2014;

Soltani et al. 2020). First, classical PCA was utilized for extracting the common factors. Then, varimax method was used for rotation and factors with eigenvalues of  $>1$  were retained for interpretation (Davis 2002). In addition, threshold value of 0.3-0.6 for loadings in factor analysis was considered to extract significant multi-elemental signature of the ore-type sought (Li in this paper). These loading values are proper criteria for separation of factors and their components with lower noises in a factor analysis (Davis 2002).

The SFA is based on two operations including rejection of noise elements and selection of main factors for further factor analysis (Yousefi et al. 2014; Afzal et al. 2019; Mirzaei et al. 2020; Soltani et al. 2020). The obtained factor scores are optimum and proper for geochemical interpretation. Noise elements are not existed in the any groups. First of all, the noise elements should be removed in a case study. In the next phase, major factors related to the ores or mineralization type have to selected and factor analysis (Fyzollahi et al. 2018; Saadati et al. 2020; Soltani et al. 2020). In this study, factor of Li is important for geochemical exploration.

### 2.3. Dataset

In this research, 4423 stream sediment samples were collected by Jianxi Chinese Company from three 1:100000 geological sheets at 1995 and were analyzed by Inductively Coupled Plasma Mass Spectrometry (ICP-MS) method by AMDEL Co. (Australia). For Quality assurance (Qa) and Quality control (Qc), 236 duplicate samples were collected and analyzed. The T-student and Fisher tests were carried out for validation of data in 95% confidence level. The studied region has dimensions equal to 140 km  $\times$  90 km, as depicted in Fig 1. For sampling, four samples were collected from each two km<sup>2</sup> and all of them were mixed for preparation of one index sample. Consequently, there is a symmetrical sampling grid.

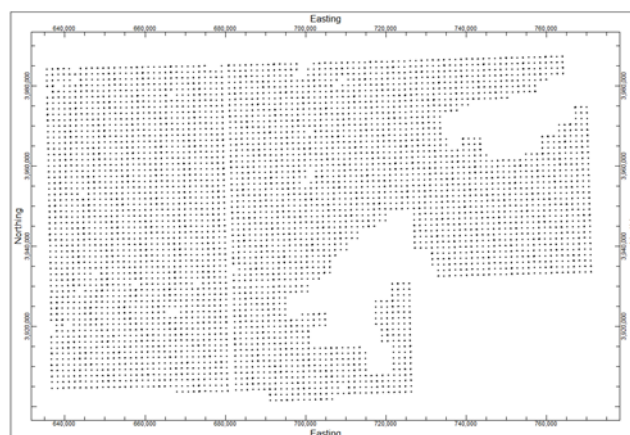


Fig 1. The sampling grid in the studied region

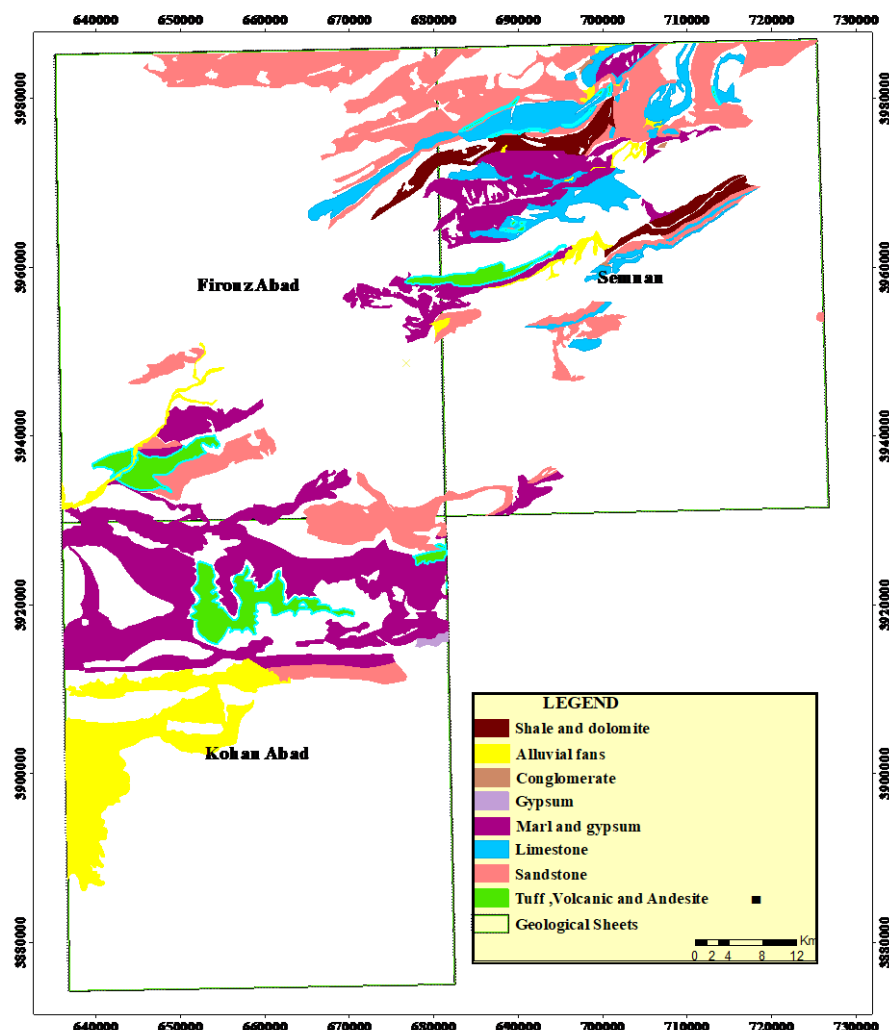


Fig. 2. Geological map of this study region which is modified based on Nabavi (1987) and Aghanabati (2004).

### 3. Geological setting

The study region is situated in the northern part of central Iran structural zone including Semnan, Kohan abad and Firouz abad 1:100000 sheets (Fig 2). There are many structures and faults which were occurred in the Silurian-Late Cenozoic (Nabavi 1987). This region is covered by major sedimentary and minor Middle Eocene volcanic units, belonging to the Karaj Formation (Nabavi 1987; Aghanabati 2004). The volcano-sedimentary sequence is mainly composed of tuff and shale (E), andesite-dacite-rhyolite, interlayers of volcanic rocks and shale, dacitic tuff and rhyolitic tuff (Fig 1) which are mostly altered (Nabavi 1987; Mahdavi et al. 2015; Yazdi et al. 2017, 2019). This sequence is dominantly intruded by felsic to intermediate bodies with small outcrops. Marl, sandstones, clay minerals and gypsum are abundant in this district, as depicted in Fig 2.

The volcano sedimentary and intrusive rocks exhibit alteration assemblages which are generally verified by the field studies and laboratory analysis. The alteration minerals comprise mainly chlorite, hematite and

limonite in andesites and dacites. Alteration of felsic rocks is represented by the clay minerals and iron oxides as well as alunite and jarosite (Modabberi et al. 2017). There are many sedimentary mineralization such as borates, different salts, sodium sulfates, gypsum, kaolinites and coal. Moreover, Pb-Zn and Cu occurrences exist in this region. Existence of alunite and jarosite neighboring to the magmatic outcrops of felsic rocks could be considered as an important evidence for detailed exploration of Au, and Cu in this region (Modabberi et al. 2017).

### 4. Results and Discussion

#### 4.1. Statistical analysis

First, a statistical analysis was carried out using conventional methods based on mean median and Standard Deviation (SD). Mean, median and SD for lithium are 32.1 ppm, 30 ppm and 11.51 ppm, respectively. The Li distribution is not normal based on its histogram, as depicted in Fig 3.

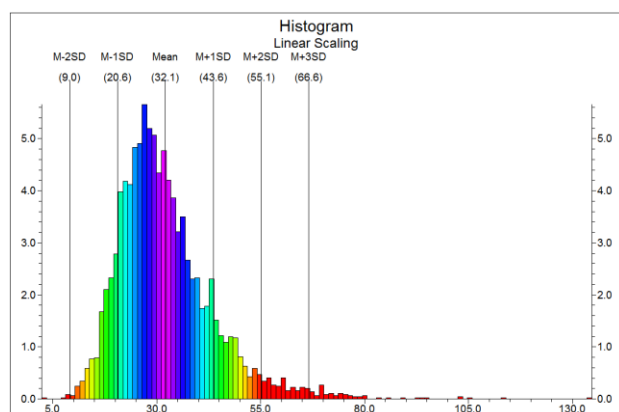


Fig. 3. Li histograms for stream sediments data in the studied region

On the other hand, data distribution is not normal and similar to lognormal type. Based on the abnormal distribution for Li, median should be used (Davis 2002). Based on this position, threshold values for Li can be calculated based on median and its summation with standard deviation. Threshold values equal to 30 ppm, 41.51 ppm, 53.02 ppm and 64.53 ppm which are median, median + SD, median + 2SD and median + 3SD, respectively.

#### 4.2. Application of SFA

The stream sediment data should be opened based on compositional nature of them. Simple approach for this work is a logarithmic transformation based on Napierian digit (Ln). The SFA was utilized for factors extraction based on the 29 ln-transformed elemental concentration data. However, the varimax rotation of factors was applied by the SPSS software. In the first step, the factor analysis scores with greater than 0.6 were selected (Table 1). Bi, As, Sb, Sn, Sr, Hg and W were rejected in this stage, as depicted in Table 1. In the second stage, Ba and Au were removed, as depicted in Table 2. All elements did not removed in third stage because all scores more than 0.6, as depicted in Table 3. Factor related to Li are F1-3 and F2-3 which were selected for final stage of factor analysis. Results obtained by the SFA shows that Li paragenesis are B, Cs, F, U and Rb, as depicted in Table 4. B is an index element for lithium accumulation in the clay minerals and also, Cs, F, U and Rb (F2-4) can be shown a magmatic source for lithium (Kesler et al. 2012) in this region such as studies of Fyzollahi et al. (2018) and Saadati et al. (2020). Loading plot of the final stage represents two final factor which is shows Li with other paragenesis elements in this district (Fig 4).

#### 4.3. S-A fractal model

In this step, F2-4 was classified by the S-A fractal modeling, as depicted in Fig 5. First, the F2-4 scores were interpolated by Advanced Inverse Distance Squared (AIDS) method by RockWorks 15 software package. Then, the estimated factor scores were transformed to

power spectrum by a MATLAB code which is introduced by Afzal et al. (2012 and 2013). The obtained results presented five populations within multifractal nature for F2-4 data (Fig 5). First right-hand population with log SA < -0.25 shows noise data, as depicted in Fig 5.

Table 1. First stage of the SFA

	Rotated Component Matrix <sup>a</sup>						
	Component						
	1	2	3	4	5	6	7
Na <sub>2</sub> O	.045	-.029	.012	-.047	-.046	<b>.849</b>	.034
Zn	.287	.169	<b>.763</b>	.133	.076	.058	.038
Pb	-.043	.038	<b>.823</b>	.083	.024	.016	.011
Ag	.173	-.087	.648	-.137	.345	-.074	-.153
Cr	<b>.908</b>	.097	-.012	.188	-.085	-.051	.026
Ni	<b>.877</b>	.083	.049	.032	.018	-.105	-.036
Bi	.022	.259	-.126	.143	.410	-.008	-.277
Cu	<b>.832</b>	.179	.101	-.015	.151	.033	-.025
As	.049	.405	.222	.451	.215	.136	.118
Sb	.038	-.027	.052	-.115	.500	-.003	.279
Co	<b>.906</b>	.175	.040	.098	.106	.095	.031
Sn	.414	.153	.013	.203	.275	-.112	-.293
Ba	.118	-.065	.231	-.061	<b>.605</b>	.198	-.079
V	<b>.878</b>	.207	.093	.079	.128	.134	.023
Sr	-.370	-.133	-.182	-.566	-.055	.254	-.043
Hg	.111	.136	.105	.084	.484	-.071	.087
W	.068	.162	-.080	.219	.148	.146	-.009
B	.051	<b>.716</b>	.025	.065	-.185	.206	.024
Be	<b>.753</b>	.485	.056	.161	.201	.049	-.069
Mo	-.214	.146	-.017	<b>-.812</b>	.141	.078	.022
Li	.351	<b>.751</b>	-.058	.186	-.003	.066	.008
Au	-.009	.033	-.068	.074	.128	-.022	<b>.807</b>
Rb	.367	<b>.766</b>	.079	.251	.185	.009	-.070
P	<b>.758</b>	.063	.220	.008	.024	.069	.000
Cs	.146	<b>.696</b>	.034	.189	.306	-.187	-.225
Nb	<b>.861</b>	.164	-.014	.113	.117	.078	-.025
Th	.177	.456	.058	-.049	.253	.538	-.104
U	.131	<b>.667</b>	.011	-.399	.095	-.034	.100
F	.259	<b>.699</b>	.116	-.330	.051	-.105	.038

Table 2. Second stage of the SFA

Rotated Component Matrix<sup>a</sup>

	Component				
	1	2	3	4	5
Na <sub>2</sub> O	.077	-.094	.042	.158	<b>.915</b>
Zn	.267	.207	<b>.729</b>	-.127	.055
Pb	-.076	.087	<b>.777</b>	-.171	.013
Ag	.140	-.058	<b>.749</b>	.134	-.078
Cr	<b>.903</b>	.145	-.032	-.189	-.037
Ni	<b>.863</b>	.115	.066	-.050	-.140
Cu	<b>.833</b>	.180	.161	.105	-.035
Co	<b>.922</b>	.187	.080	-.004	.020
Ba	.159	-.042	.481	.271	-.017
V	<b>.889</b>	.214	.136	.029	.099
B	.036	<b>.701</b>	-.065	.048	.359
Be	<b>.761</b>	.518	.127	.018	.000
Mo	-.230	-.051	.012	<b>.850</b>	-.019
Li	.350	<b>.785</b>	-.078	-.032	.093
Au	-.018	.041	-.015	-.058	.186
Rb	.366	<b>.824</b>	.122	-.019	.030
P	<b>.744</b>	.070	.229	.025	.110
Cs	.142	<b>.694</b>	.157	-.055	-.216
Nb	<b>.875</b>	.179	.043	-.009	-.008
U	.122	.531	-.016	<b>.610</b>	-.042
F	.221	<b>.632</b>	.091	.444	-.035

Table 3. Third stage of the SFA

Component Matrix<sup>a</sup>

	Component				
	1	2	3	4	5
Na <sub>2</sub> O	.047	.015	-.015	.455	<b>.832</b>
Zn	.463	-.084	<b>.681</b>	-.095	.106
Pb	.118	-.059	<b>.799</b>	-.163	.093
Ag	.231	-.136	<b>.709</b>	.114	-.080
Cr	<b>.836</b>	-.352	-.205	-.034	-.034
Ni	<b>.806</b>	-.316	-.096	.044	-.162
Cu	<b>.832</b>	-.189	-.009	.161	-.095
Co	<b>.895</b>	-.255	-.124	.096	-.016
V	<b>.894</b>	-.207	-.049	.143	.051
B	.363	<b>.687</b>	-.073	-.090	.366
Be	<b>.924</b>	.078	-.048	-.052	-.005
Mo	-.201	.417	.137	<b>.701</b>	-.277
Li	<b>.662</b>	.470	-.161	-.229	.125
Rb	<b>.729</b>	.474	.012	-.274	.085
P	<b>.718</b>	-.271	.085	.181	.066
Cs	.475	<b>.634</b>	.075	-.402	-.117
Nb	<b>.844</b>	-.242	-.142	.084	-.043
U	.370	<b>.623</b>	.028	.351	-.221
F	.519	<b>.679</b>	.091	.182	-.149

Table 4. Fourth (Final) stage of the SFA

Rotated Component Matrix<sup>a</sup>

	Component	
	1	2
Cr	<b>0.911</b>	0.113
Ni	<b>0.872</b>	0.116
Cu	<b>0.831</b>	0.228
Co	<b>0.921</b>	0.208
V	<b>0.889</b>	0.252
B	0.014	<b>0.706</b>
Be	<b>0.759</b>	0.533
Li	0.332	<b>0.761</b>
Rb	0.365	<b>0.813</b>
P	<b>0.752</b>	0.116
Cs	0.17	<b>0.646</b>
Nb	<b>0.873</b>	0.194
U	0.051	<b>0.672</b>
F	0.176	<b>0.737</b>

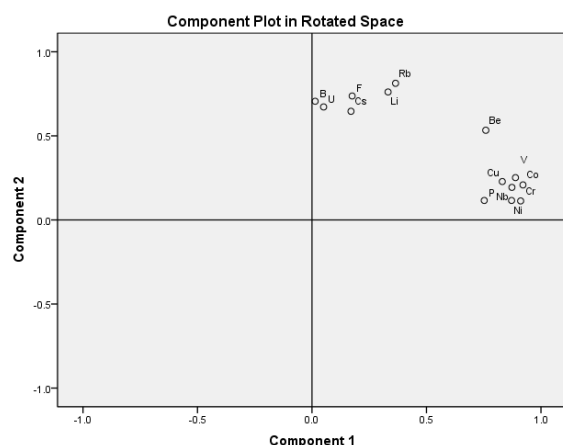


Fig. 4. Loading plot in the final stage of the SFA

The data were back-transformed by the IFFT and final anomaly map was created for the F2-4. Background and main anomaly are  $\leq 0.6$  and  $\geq 1.5$  for F2-4, respectively. Main anomalous areas are located in the SW, northern and eastern part of the studied area as depicted in Fig 6.

#### 4.4. Validation with further rock samples

There are 14 litho-geochemical samples which were collected for validation of Li anomalies. These samples were used for validation of research. There are five samples with Li concentration higher than 100 ppm. These samples have good correlation with main anomalies of  $F2-4 \geq 1.5$ , as depicted in Fig 7. All of these

samples ( $Li \geq 100$  ppm) were situated in the F2-4 anomalies at the northern (Semnan and Firouz Abad) and SW (Koahan Abad) parts of the study area.

In addition, these anomalies were correlated with lithological types in this step. The extreme anomaly of F2-4 ( $\geq 3.2$ ) is associated with andesites, tuffs and black shales in the SW part of this district, as depicted in Fig 8. Furthermore, there are a good correlation between main anomalies of F2-4 and marls, clay minerals, dolomites and limestones in the northern and eastern parts of this area (Fig 9). Based on adjacent to Alborz mountains, these anomalies can be achieved by the plutonic rocks especially granitic-pegmatitic rocks.

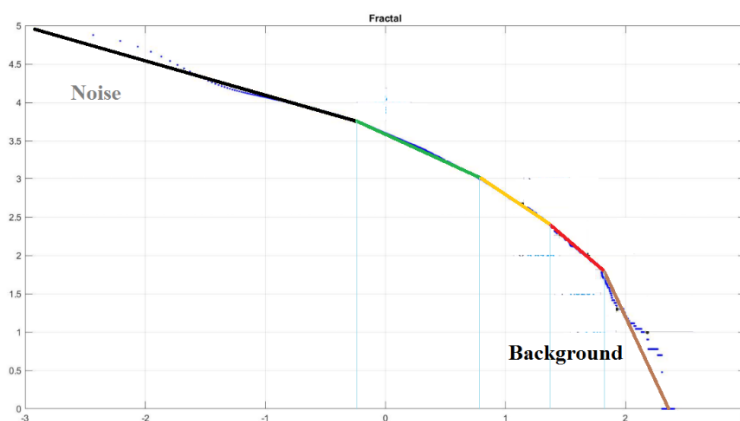


Fig 5. S-A log-log plots for F2-4

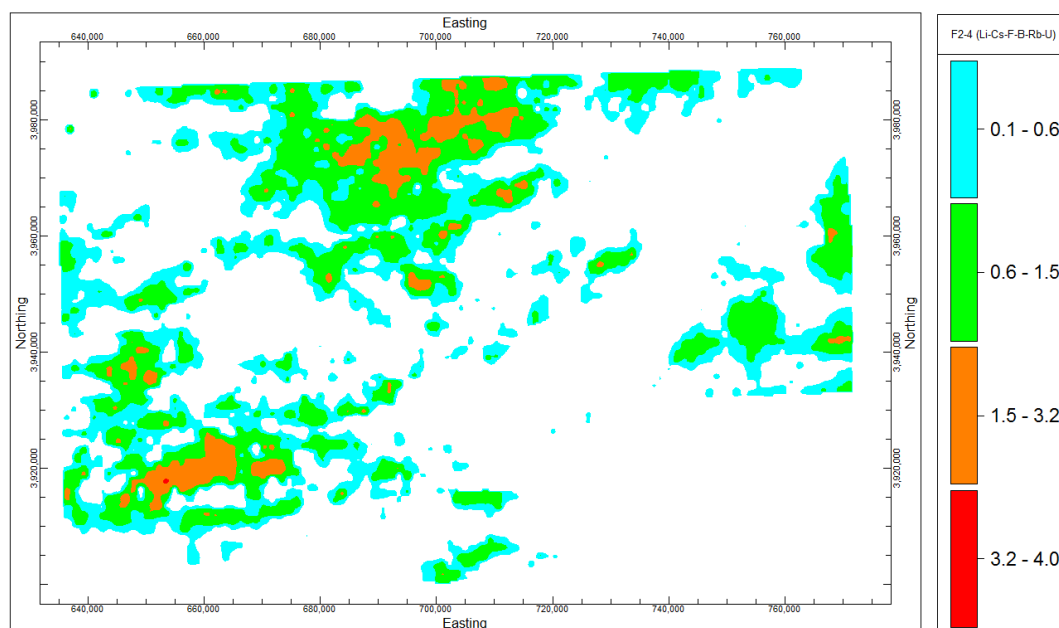


Fig 6. Distribution maps for F2-4 anomalies based on the S-A fractal model

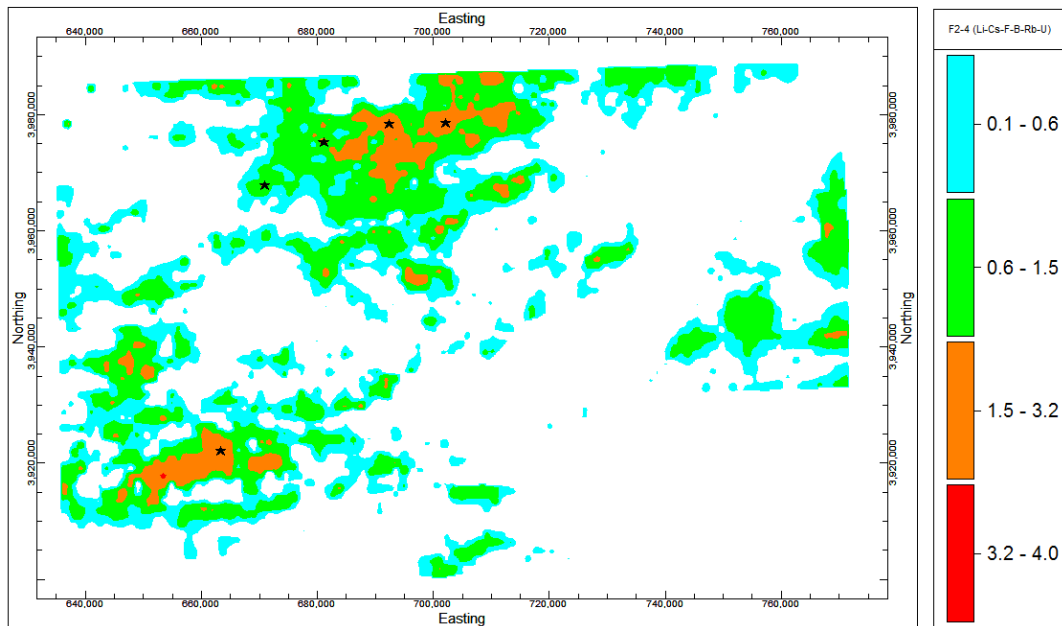


Fig 7. Correlation between rock samples with  $Li \geq 100$  ppm (black stars) and the F2-4 anomalies based on the S-A fractal model

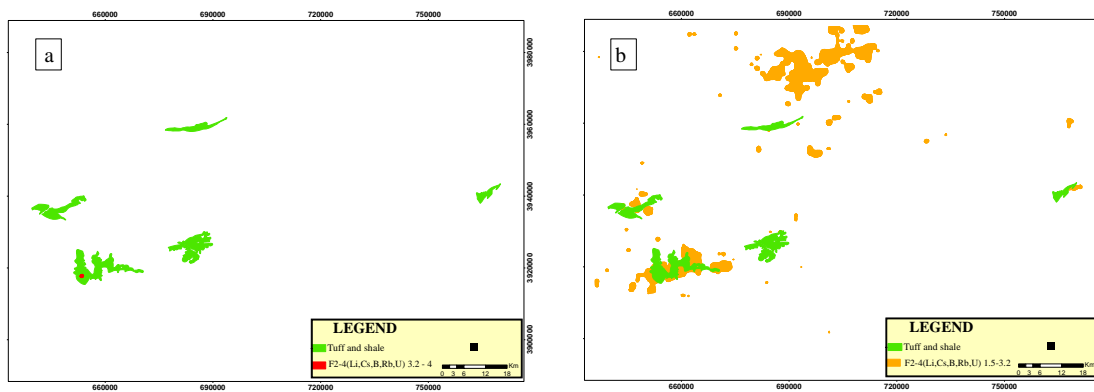


Fig. 8. Correlation between (a) the extreme F2-4 anomalies ( $\geq 3.2$ ) and (b) the main F2-4 anomalies ( $\geq 1.5$ ) derived via the fractal model with tuffs and black shales

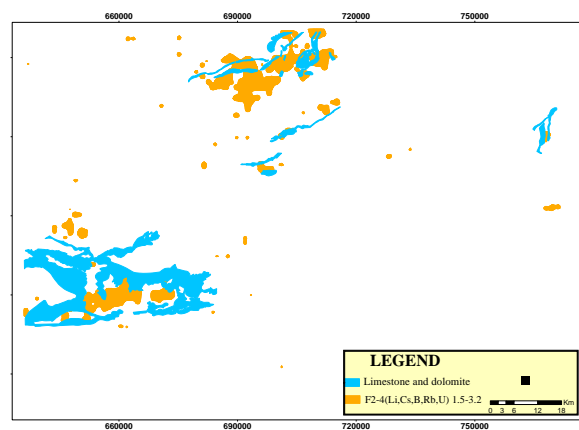


Fig. 9. Correlation between the main F2-4 anomalies ( $\geq 1.5$ ) derived via the fractal model with dolomite, limestone, marl and clay minerals

## 5. Conclusion

Results of this study denote that this combination technique is effective for regional exploration (reconnaissance in this study) especially for rare metals as lithium. Based on the SFA, paragenesis of the target element (Li with B-Cs-Rb-U as F2-4 in this scenario) can be detected which is a suitable method for recognition of ore element anomalies. These elements can indicate a granitic source for Li mineralization such as previous works in Iran. Moreover, the S-A fractal modeling is helped for de-noise of data and better interpretation. The F2-4 values higher than 1.5 represent main anomalies in the study area. In this research, Li anomalies derived via the fractal-SFA model are correlated with geological particulars of lithium mineralization and further rock samples. Major anomalies of F2-4 can be indicated lithium mineralization of granitic-pegmatitic type in the SW (Kohan Abad 1:100000 sheet) and northern parts and Li resources with clay minerals in the northern sector of the studied area which are Semnan and Firouz Abad. On the other hand, the SW and northern parts have proper potential for next stages of exploration operation. Accumulation of Li with B, Cs, Rb and U can be indicated a granitic pegmatite mineralization potential in this region. Moreover, several anomalies exist in the marls and clay minerals which can be a potential for future exploration projects.

## Acknowledgement

Authors would like to thank Geological Survey of Iran (GSI) for preparation of datasets. Furthermore, authors acknowledge Dr. Behzad Behbahani for his contribution for data gathering and interpretation.

## Reference

- Afzal P, Ahmadi K, Rahbar K (2017a) Application of fractal-wavelet analysis for separation of geochemical anomalies. *Journal of African Earth Sciences* 128: 27-36.
- Afzal P, Alghalandis YF, Moarefvand P, Omran NR, Haroni HA (2012) Application of power-spectrum-volume fractal method for detecting hypogene, supergene enrichment, leached and barren zones in Kahang Cu porphyry deposit, Central Iran. *Journal of Geochemical Exploration* 112: 131-138.
- Afzal P, Harati H, Alghalandis YF, Yasrebi AB (2013) Application of spectrum-area fractal model to identify of geochemical anomalies based on soil data in Kahang porphyry-type Cu deposit, Iran. *Chemie der Erde/Geochemistry* 73: 533-543.
- Afzal P, Heidari SM, Ghaderi M, Yasrebi AB (2017b) Determination of mineralization stages using correlation between geochemical fractal modeling and geological data in Arabshah sedimentary rock-hosted epithermal gold deposit, NW Iran. *Ore Geology Reviews* 91: 278-295.
- Afzal P, Khakzad A, Moarefvand P, Omran NR, Esfandiari B, Alghalandis YF (2010) Geochemical anomaly separation by multifractal modeling in Kahang (Gor Gor) porphyry system, Central Iran. *Journal of Geochemical Exploration* 104: 34-46.
- Afzal P, Yasrebi AB, Saein LD, Panahi S (2017c) Prospecting of Ni mineralization based on geochemical exploration in Iran. *Journal of Geochemical Exploration* 181: 294-304.
- Afzal P, Yusefi M, Mirzaie M, Ghadiri-Sufi E, Ghasemzadeh S (2019) Delineation of podiform-type chromite mineralization using Geochemical Mineralization Prospectivity Index (GMPI) and staged factor analysis in Balvard area (southern Iran). *Journal of Mining and Environment* 10, 705-715.
- Aghanabati A (2004) Geology of Iran. Geological Survey of Iran Publication. 586 p (in Persian).
- Agterberg FP, Cheng Q, Brown A, Good D. Multifractal (1996) Multifractal modeling of fractures in the Lac du Bonnet batholith, Manitoba. *Computers and Geosciences* 22 (5), 497-507.
- Shahsavari MA, Afzal P, Hekmatnejad A (2020) Identification of geochemical anomalies using fractal and LOLIMOT neuro-fuzzy modeling in Mial area, Central Iran. *Journal of Mining and Environment* 11: 99-117.
- Chen G, Cheng Q (2018) Fractal-Based Wavelet Filter for Separating Geophysical or Geochemical Anomalies from Background. *Mathematical Geosciences* 50: 249-272.
- Cheng Q (1999) Spatial and scaling modelling for geochemical anomaly separation. *Journal of Geochemical Exploration* 65 (3): 175-194.
- Cheng Q, Agterberg FP, Ballantyne SB. (1994) The separation of geochemical anomalies from background by fractal methods. *Journal of Geochemical Exploration* 51: 109-130.
- Daneshvar Saein L, Rasa I, Rashidnejad Omran N, Moarefvand P, Afzal P (2012) Application of concentration-volume fractal method in induced polarization and resistivity data interpretation for Cu-Mo porphyry deposits exploration, case study: Nowchun Cu-Mo deposit, SE Iran. *Nonlinear Processes in Geophysics* 19: 431-438.
- Daneshvar Saein L, Rasa I, Rashidnejad Omran N, Moarefvand P, Afzal P (2014) Application of number-size (N-S) fractal model to quantify of the vertical distributions of Cu and Mo in Nowchun porphyry deposit (Kerman, SE Iran). *Archives of Mining Sciences* 58: 1, 89-105.
- Daneshvar Saein L, Afzal P (2017) Correlation between Mo mineralization and faults using geostatistical and fractal modeling in porphyry deposits of Kerman Magmatic Belt, SE Iran. *Journal of Geochemical Exploration* 181: 33-343.
- Davis JC (2002) Statistics and data analysis in Geology (3th ed.). John Wiley & Sons Inc., New York.
- Farahmandfar Z, Jafari MR, Afzal P, Ashja Ardalan A (2020) Description of gold and copper anomalies using



- fractal and stepwise factor analysis according to stream sediments in NW Iran. *Geopersia* 10 (1):135-148.
- Fyzollahi N, Torshizian H, Afzal P, Jafari MR (2018) Determination of lithium prospects using fractal modeling and staged factor analysis in Torud region, NE Iran. *Journal of Geochemical Exploration* 189: 2-10.
- Ghasemzadeh S, Maghsoudi A, Yousefi M, Mihalasky MJ (2019) Stream sediment geochemical data analysis for district-scale mineral exploration targeting: Measuring the performance of the spatial U-statistic and C-A fractal modeling. *Ore Geology Reviews* 113: 103115.
- Gourcerol B, Gloaguen E, Melleton J, Tuduri J, Galiegue X (2020) Re-assessing the European lithium resource potential – A review of hard-rock resources and metallogeny. *Ore Geology Reviews* 109: 494-519.
- Hawkes HE, Webb JS (1979) *Geochemistry in mineral exploration*, 2nd ed. *Academic Press*, New York, 657 p.
- Hassanpour Sh, Afzal P (2013) Application of concentration-number (C-N) multifractal modelling for geochemical anomaly separation in Haftcheshmeh porphyry system, NW Iran. *Arabian Journal of Geosciences* 6: 957–970.
- Heidari M, Ghaderi M, Afzal P (2013) Delineating mineralized phases based on litho-geochemical data using multifractal model in Touzlar epithermal Au-Ag (Cu) deposit, NW Iran. *Applied Geochemistry* 31: 119-132.
- Kesler SE, Gruber PW, Medina PA, Keoleian GA, Everson MP, Wallington TJ (2012) Global lithium resources: Relative importance of pegmatite, brine and other deposits. *Ore Geology Reviews* 48: 55–69.
- Khalili H, Afzal P (2018) Application of spectrum-volume fractal modeling for detection of mineralized zones. *Journal of Mining and Environment* 9: 371-378.
- London D (2008) Pegmatites. *Can. Mineral. Spec. Publ.* 10, 347.
- Mahdavi M, Dabiri R, Hosseini ES (2015) Magmatic evolution and compositional characteristics of tertiary volcanic rocks associated with the Venarch manganese mineralization, SW Qom, central Iran. *Earth Sciences Research Journal* 19(2):141-5.
- Mandelbrot BB (1983) *The Fractal Geometry of Nature*: W. H. Freeman. San Fransisco, 468 p.
- Mirzaei M, Afzal P, Adib A, Rahimi E, Mohammadi Gh (2020) Detection of zones based on ore and gangue using fractal and multivariate analysis in Chah Gaz iron ore deposit, Central Iran. *Journal of Mining and Environment* 11(2), 453-466.
- Modabberi S, Ahmadi A, Tangestani MH (2017) Sub-pixel mapping of alunite and jarosite using ASTER data; a case study from north of Semnan, north central Iran. *Ore Geology Reviews* 80: 429-436.
- Nabavi MH (1987) 1:100,000 geological map of Semnan Geological Survey of Iran.
- Ostadosseini A, Barati M, Afzal P, Lee I. (2018) Polymetallic mineralization prospecting using fractal and staged factor analysis in Ardestan area, Central of Iran. *Geopersia* 8: 279-292.
- Reimann C, Filzmoser P, Garrett RG (2005) Background and threshold: critical comparison of methods of determination. *Science of the Total Environment* 346: 1–16.
- Saadati H, Afzal P, Torshizian H, Solgi A (2020) Geochemical exploration for Li using Geochemical Mapping Prospectivity Index (GMPI), fractal and Stage Factor Analysis (SFA) in NE Iran. *Geochemistry: Exploration, Environment, Analysis* (In press).
- Soltani F, Moarefvand P, Alinia F, Afzal P (2020) Detection of Main Rock Type for Rare Earth Elements (REEs) Mineralization Using Staged Factor and Fractal Analysis in Gazestan Iron-Apatite Deposit, Central Iran. *Geopersia* 10(1): 89-99.
- Yazdi A, Shahhosini E, Dabiri R, Abedzadeh H (2019) Magmatic differentiation evidences and source characteristics using mineral chemistry in the Torud intrusion (Northern Iran). *Revista Geoaraguaia* 9(2): 1-21.
- Yazdi A, Ashja-Ardalan A, Emami MH, Dabiri R, Foudazi M (2017) Chemistry of Minerals and Geothermobarometry of Volcanic Rocks in the Region Located in Southeast of Bam, Kerman Province. *Open Journal of Geology* 7(11): 1644-1653.
- Yousefi M, Kamkar-Rouhani A, Carranza EJ (2012) Geochemical mineralization probability index (GMPI): A new approach to generate enhanced stream sediment geochemical evidential map for increasing probability of success in mineral potential mapping. *Journal of Geochemical Exploration* 115: 24-35.
- Yousefi M, Kamkar-Rouhani A, Carranza EJ (2014) Application of staged factor analysis and logistic function to create a fuzzy stream sediment geochemical evidence layer for mineral prospectivity mapping. *Geochemistry: Exploration, Environmental, Analysis* 14: 45-58.
- Yousefi M, Kreuzer OP, Nykänen V, Hronsky JM (2019) Exploration information systems – A proposal for the future use of GIS in mineral exploration targeting. *Ore Geology Reviews* 111: 103005.
- Zuo R (2014) Identification of geochemical anomalies associated with mineralization in the Fanshan district, Fujian, China. *Journal of Geochemical Exploration* 139: 170–176.
- Zuo R, Wang J (2016) Fractal/multifractal modeling of geochemical data: A review. *Journal of Geochemical Exploration* 164: 33-41.